Bioorganic Chemistry 114 (2021) 105068

Contents lists available at ScienceDirect

Bioorganic Chemistry

journal homepage: www.elsevier.com/locate/bioorg

Investigation of indole functionalized pyrazoles and oxadiazoles as anti-inflammatory agents: Synthesis, *in-vivo*, *in-vitro* and *in-silico* analysis

Devendra Kumar [a,2], Ravi Ranjan Kumar [a,2], Shelly Pathania [a,1], Pankaj Kumar Singh [b], Sourav Kalra [c], Bhupinder Kumar [a,*]

[a] Department of Pharmaceutical Chemistry, ISF College of Pharmacy, Ghal Kalan, Ferozpur G.T. Road MOGA-142001, Punjab, India
[b] Integrative Physiology and Pharmacology, Institute of Biomedicine, Faculty of Medicine, University of Turku, FI-20520 Turku, Finland
[c] Department of Pharmaceutical Technology (Process Chemistry), National Institute of Pharmaceutical Education and Research, SAS Nagar, Sector 67, Mohali, Punjab 160062, India

ARTICLE INFO

Keywords:
Anti-inflammatory
Antioxidants
Indole derivatives
Oxadiazole derivatives
COX-2 inhibitors

ABSTRACT

There are several potential side and adverse effects are found to be associated with the anti-inflammatory drugs in clinical practice. The long-term use of these clinical agents highly unsafe. It encouraged the development of novel heterocyclic compounds with potential anti-inflammatory activity and low to no toxicity. In present investigation, a total of 12 indole functionalized pyrazole and oxadiazole derivatives were designed, synthesized and evaluated for the in-vivo anti-inflammatory and analgesic potential. These compounds displayed comparable anti-inflammatory and analgesic potential to the reference drugs. Finally, molecular docking analysis was performed considering different anti-inflammatory targets to determine the mechanistic target of the designed molecules. Detailed analysis suggested that the molecules inhibit COX-2, preferably over other anti-inflammatory targets. The results suggested that two compounds (15c and 15f) were found promising candidates for the development of novel anti-inflammatory agents.

1. Introduction

Inflammation is a protective mechanism that defends the human body from any injury or damage to its cells by any harmful foreign particles or stimuli [1–4]. Pain, heating sensation, swelling, and redness are major signs of inflammation in any tissue which ultimately alters the tissue function [5]. During inflammation, various microcirculatory events take place such as white blood cell recruitment, alteration in vascular permeability, production and release of pro-inflammatory/inflammatory mediators, tissue destruction etc. [6,7]. Interleukin (IL)-1β is one of the key inflammatory mediators and helps in production of potent pro-inflammatory cytokines [8,9]. It helps in various acute phase inflammation reactions in body [10]. In case of acute inflammation, body can restore tissue homeostasis and its functions [11], but in some cases, it becomes chronic and continuous inflammatory condition affects the tissue and body functions of a person to great extent. In cases where IL-1β level is low, the release of adrenocorticotropic hormone and formation of cytokines such as IL-6 is triggered which leads to overexpression of hepatic acute-phase proteins such as serum amyloid A and C-reactive protein. It leads to the leucocytosis and thrombocytosis processes and causes the synthesis of adhesion molecules in endothelial cells [12]. Arachidonic acid is another key component present in cell membranes which causes the activation of other key inflammatory mediator known as eicosanoids [13,14]. Other inflammatory mediators also include 5-lipoxygenase, 12- lipoxygenase, and cyclooxygenase [15,16]. Steroidal anti-inflammatory drugs are the first class of drugs used for the treatment of inflammation but use of these drugs is associated with severe side/adverse effects [17]. These adverse effects are reduced or minimized by non-steroidal anti-inflammatory drugs (NSAIDs) but other adverse effects such as gastric ulcers and renal function impairments mark questions on their use [18–20]. Such problems associated with NSAIDs were fixed by the discovery of selective COX-2 inhibitors [21,22] but long-term use of these COX-2 inhibitors produced serious side effects such as cardiovascular complications [23,24] due to decreased level of anti-thrombotic prostaglandins [25,26].

* Corresponding author.
E-mail addresses: shellpathania91@gmail.com (S. Pathania), bhupinderkumar@isfcp.org (B. Kumar).
[1] Co-corresponding author.
[2] Both authors have equal contribution.

https://doi.org/10.1016/j.bioorg.2021.105068
Received 22 May 2021; Received in revised form 1 June 2021; Accepted 5 June 2021
Available online 8 June 2021

From NSAIDs, Indomethacin is one of the most promising anti-inflammatory agents. It is found to possess good potency in the treatment of various inflammatory disorders such as rheumatoid arthritis, ankylosing spondylitis, osteoarthritis etc. However, it is also associated with serious gastric ulcer problems due to its acidic nature and high affinity for COX-1 inhibition. Thus, the development of new potential anti-inflammatory drug molecules with no or minimal adverse effect is still a need of the hour. Despite hard work and exhaustive research efforts worldwide a set of enormously important fundamental questions associated with inflammation mechanism is unresolved [27]. In case of indomethacin, one strategy to minimize adverse effects is to perform structural modifications at acid group present at C3 position while retaining the indole pharmacophore. From literature survey, it is found that structural modification at C3 position of 2-phenylindole presents a potent pharmacophore for anti-inflammatory drug development. The resultant compounds are sought to possess more potent anti-inflammatory and antioxidant properties and improved LOX inhibition [28]. On other hand, Celecoxib, containing pyrazoline moiety, is a well-known selective COX-2 inhibitor used for the treatment of inflammation [29,30]. The anti-inflammatory and pain-relieving properties of celecoxib result from inhibition of prostaglandin (PG) synthesis by selective inhibition of PG G/H synthase-2 (encoded by gene PTGS2). Similarly, 1,3,4-oxadiazole is also found to possess significant anti-inflammatory potential [31,32]. 2-Aryl-5-subtituted-1,3,4-oxadiazole is a key pharmacophoric component with anti-inflammatory activity [33–35]. Thus, considering the above-mentioned information and taking forward the ongoing research efforts related to the design and development of potent anti-inflammatory agents, we designed and synthesized a library of indole functionalized pyrazole and oxadiazole derivatives, as described in Fig. 1. Further, we evaluated them for their anti-inflammatory potential along with analgesic and antioxidant properties. Finally, in-silico analysis was performed to better understand the binding modes of the designed molecules in the catalytic domain of various possible anti-inflammatory targets. Most of the compounds were found to possess moderate anti-inflammatory and analgesic properties along with a good antioxidant profile, which warrants further study of these molecules for detailed pharmacodynamics.

2. Results and discussion

2.1. Chemistry

For synthesis of pyrazoline derivatives of indole (**9a-9c**), firstly 2-phenylindole-3-carboxaldehyde (**5**) was prepared by reaction of acetophenone and phenylhydrazine which were further reacted with Vilsmeier-haack reagent to give **5**. It was further reacted with suitable acetophenones to synthesize chalcones (**7a, b**) which on reaction with appropriate hydrazine yielded target pyrazoline derivatives of indole (**9a-9c**) as per synthetic Scheme 1. Similarly, for synthesis of oxadiazole derivatives of indole (**15a-15i**), indole-3-acetic acid (**10**) was used as starting material. Indole-3-acetic acid (**10**) was first esterified with ethanol which on further treatment with hydrazine hydrate produced indole-3-acetic hydrazide (**13**). This indole-3-acetic hydrazide (**13**) was reacted with suitable benzoic acids in presence of $POCl_3$ under suitable conditions to give target oxadiazole derivatives of indole (**15a-15i**) as per synthetic Scheme 2. The synthesized compounds were characterized using Mass, IR, and NMR spectroscopic analysis.

3. *In-vivo* studies

3.1. Anti-inflammatory activity

Carrageenan test is greatly sensitive to clinically useful NSAIDs and has been widely accepted as a useful model to measure anti-inflammatory drugs. Carrageenan injection generated intense inflammation (edema as being the principal symptom) which peaked between 2 and 4 h and is attributed to release of inflammation related mediators, which is the moment when its maximum effect is demonstrated and the moment when the anti-inflammatory effect of the test product is best observed. The pharmacological results listed in Table 1 represents the mean changes in paw edema volume mL ± SD of animals pretreated with the reference drugs and test compounds after 1 h, 2 h and 4 h from the

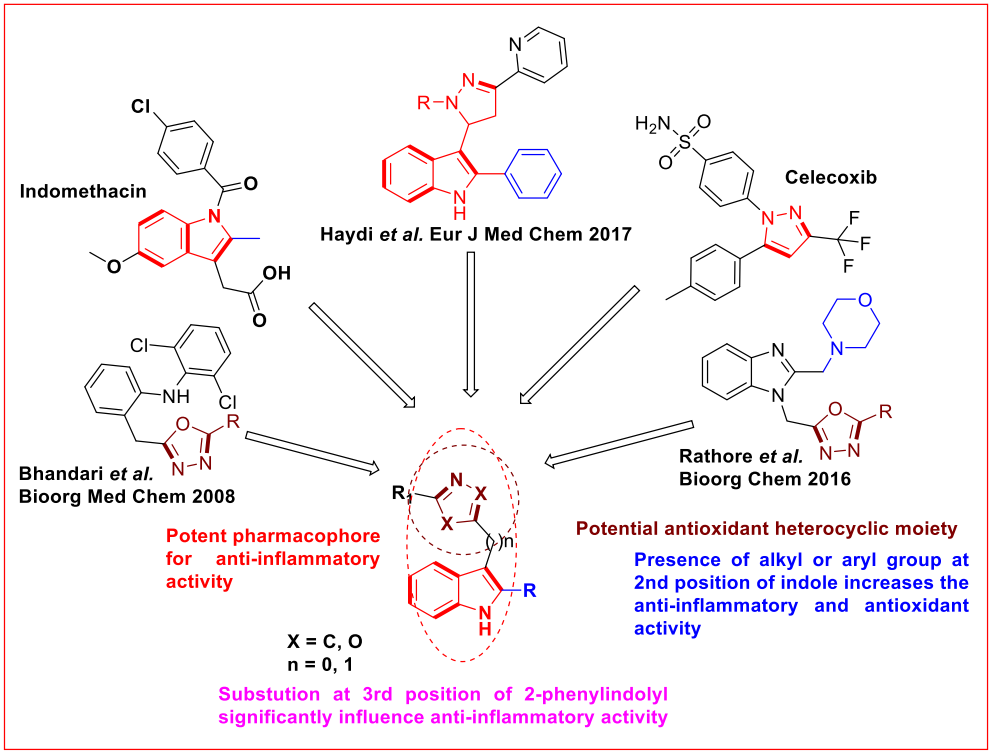

Fig. 1. Designing strategy of indole derivatives as anti-inflammatory agents.

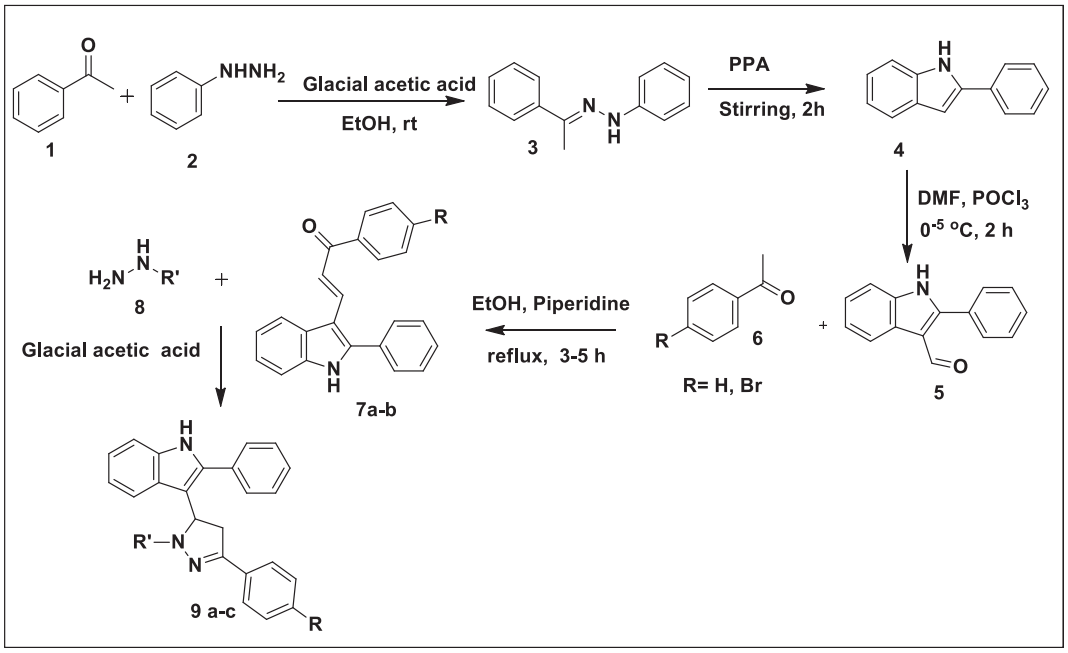

Scheme 1. Synthetic route for the synthesis of the title compounds (9a-c).

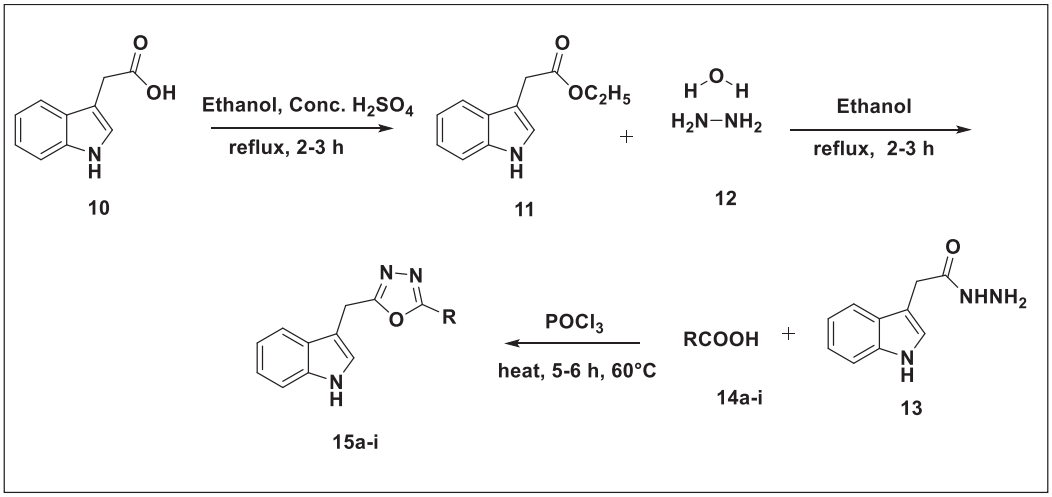

Scheme 2. Synthetic route for the synthesis of the title compounds (15a-i).

induction of inflammation, together with the percent inhibition of induced rat paw edema by the test compounds. Statistical differences of control, reference and test groups were carried out using F test (ANOVA) followed by post hoc test. The screened results revealed that strong inhibition of edema was observed after 4 h. The tested compound 15f showed significant anti-inflammatory activity (% edema reduction = 74.07%) comparable to that of indomethacin (92.59% edema reduction) and higher than rest of the molecules. Interestingly, after 1 h of dose administration 15b is showing the topmost % inhibition amongst all compounds in paw edema, but after 2 h there is not much improvement in the % inhibition value which suggests that the compound might have been inactivated/metabolised. 15b is having unsubstituted aryl ring which could be more prone to metabolism and probably, therefore it is showing lower activity after 4 h.

3.2. Analgesic activity

Tail-flick method was used to determine the analgesic potential of the compounds. A significant reduction of painful sensation due to tail immersion in warm water was observed following the administration of the test compounds. The effect was prominently noticed after a latency period of 2 h. Overall, the reaction time significantly increased in rats receiving the test compounds 15c and 15f indicating a potent analgesic effect. The analgesic activity of the compounds was done at the same dose as used for anti-inflammatory activity. The detailed results of the test compounds along with the positive control, diclofenac, are shown in Table 2.

3.3. In-vitro COX inhibitory activity

Considering the molecular modelling results, selected compounds (15a-i) were evaluated for *in vitro* COX inhibitory activity and their selectivity using COX inhibitor screening assay kit against ovine COX-1 and human COX-2. The percentage inhibition of enzyme at 10 μM concentration of compounds is expressed in Table 3 (n = 2). From results, it was observed that most of the compounds display COX-2

Table 1
In vivo anti-inflammatory activity of tested compounds using carrageenan-induced paw edema in rats.

Compound	Normal paw volume (mL)	Mean paw volume ± SEM (mL) and % inhibition			
		Time after carrageenan injection			
		0 h	1 h	2 h	4 h
Control	0.016 ± 0.006	0.049 ± 0.007	0.049 ± 0.008	0.046 ± 0.004	0.043 ± 0.006
Indomethacin	0.013 ± 0.004	0.042 ± 0.004 (12.12%)	0.036 ± 0.006 (30.30%)	0.033 ± 0.004 (33.34%)	0.015 ± 0.004 (92.59%)
9a	0.012 ± 0.003	0.043 ± 0.004 (6.06%)	0.038 ± 0.005 (21.21%)	0.031 ± 0.005 (36.67%)	0.027 ± 0.005 (44.44%)
9b	0.011 ± 0.005	0.044 ± 0.005 (0.0%)	0.039 ± 0.006 (15.15%)	0.035 ± 0.005 (20.0%)	0.026 ± 0.004 (44.44%)
9c	0.010 ± 0.006	0.046 ± 0.005 (-9.09%)	0.038 ± 0.004 (15.15%)	0.033 ± 0.006 (23.33%)	0.030 ± 0.007 (25.92%)
15a	0.012 ± 0.005	0.042 ± 0.006 (9.09%)	0.037 ± 0.005 (24.24%)	0.034 ± 0.004 (26.67%)	0.028 ± 0.006 (40.74%)
15b	0.013 ± 0.007	0.045 ± 0.005 (3.03%)	0.035 ± 0.006 (38.88%)	0.033 ± 0.005 (33.34%)	0.026 ± 0.005 (51.85%)
15c	**0.011 ± 0.005**	**0.039 ± 0.005 (15.15%)**	**0.036 ± 0.005 (24.24%)**	**0.026 ± 0.006 (50.0%)**	**0.021 ± 0.007 (62.96%)**
15d	0.012 ± 0.003	0.041 ± 0.006 (12.12%)	0.039 ± 0.007 (18.18%)	0.035 ± 0.004 (23.33%)	0.025 ± 0.006 (51.85%)
15e	0.010 ± 0.005	0.043 ± 0.004 (0.0%)	0.037 ± 0.004 (18.18%)	0.034 ± 0.005 (20.0%)	0.024 ± 0.004 (48.14%)
15f	**0.013 ± 0.003**	**0.038 ± 0.004 (24.24%)**	**0.035 ± 0.006 (33.33%)**	**0.024 ± 0.005 (63.34%)**	**0.020 ± 0.006 (74.07%)**
15g	0.011 ± 0.006	0.040 ± 0.005 (12.12%)	0.037 ± 0.007 (21.21%)	0.031 ± 0.003 (33.34%)	0.027 ± 0.003 (40.74%)
15h	0.012 ± 0.004	0.041 ± 0.005 (12.12%)	0.038 ± 0.005 (21.21%)	0.034 ± 0.006 (26.67%)	0.029 ± 0.003 (37.03%)
15i	0.013 ± 0.005	0.042 ± 0.007 (12.12%)	0.036 ± 0.006 (30.3%)	0.032 ± 0.007 (36.67%)	0.028 ± 0.006 (44.44%)

selectivity except compounds 15h and 15i which were found to be COX-1 selective. Compound 15f was found to be most selective COX-2 inhibitor with selectivity index of 2.19 followed by compound 15b (1.95). At concentration of 10 μM, compound 15c showed most potent inhibition of COX-2 with 63.23% with selectivity index of 1.49. While, 15g although has good SI but still shows low inhibitory potential against COX-2 and probably therefore it is also showing lower inhibitory potential in animal study. Another observation made is improved % inhibitory profile of 15d in animal study however, the compound showed only sub-optimal levels of inhibition in both isoforms of COX. Limited SAR explicitly indicated the structural features which could be considered responsible for the compounds which are more active against COX-2 over COX-1. In general, electron-withdrawing substituent containing compounds showed an improved COX-2 inhibitory profile. While electron-donating substituent containing compounds showed less inhibition of COX-2. Compound 15a, a benzyl derivative which does not retain the planar conformation also showed poor inhibitory potential than other compounds of the class. Conversely, in case of COX-1, electron-donating substituent containing compounds (15h & 15i) fared better than electron-withdrawing substituent containing compounds. Accordingly, almost all the compounds showed good selectivity amongst COX-1 and COX-2, except for 15e, which showed similar levels of inhibition in both the isoforms.

Table 2
In vivo analgesic activity of tested compounds using tail-flick method.

Compound	Predrug (mean ± SEM) Reaction time in (*sec*)	Reaction time in *sec* (mean ± SEM)			
		30 min	1 h	2 h	3 h
Vehicle	2.58 ± 0.24	2.76 ± 0.44	2.78 ± 0.37	2.85 ± 0.23	2.82 ± 0.41
Diclofenac	**2.98 ± 0.30**	**7.50 ± 0.37**	**7.75 ± 0.47**	**8.91 ± 0.27**	**8.31 ± 0.42**
9a	2.35 ± 0.24	4.92 ± 0.31	5.30 ± 0.33	5.33 ± 0.29	5.13 ± 0.44
9b	2.11 ± 0.33	3.35 ± 0.24	4.74 ± 0.17	5.32 ± 0.22	5.11 ± 0.39
9c	2.29 ± 0.26	4.15 ± 0.11	4.97 ± 0.22	5.34 ± 0.27	5.11 ± 0.38
15a	2.17 ± 0.19	5.28 ± 0.28	4.88 ± 0.17	5.15 ± 0.26	5.07 ± 0.47
15b	2.41 ± 0.24	3.25 ± 0.14	4.77 ± 0.37	5.21 ± 0.24	4.76 ± 0.29
15c	**2.65 ± 0.29**	**4.95 ± 0.34**	**5.44 ± 0.37**	**7.69 ± 0.20**	**6.39 ± 0.37**
15d	2.39 ± 0.31	4.45 ± 0.24	4.77 ± 0.17	5.31 ± 0.29	5.03 ± 0.27
15e	2.24 ± 0.33	5.10 ± 0.44	5.24 ± 0.37	5.71 ± 0.25	5.12 ± 0.17
15f	**2.39 ± 0.17**	**4.28 ± 0.37**	**5.15 ± 0.33**	**6.98 ± 0.28**	**6.08 ± 0.47**
15g	2.35 ± 0.15	4.38 ± 0.19	4.74 ± 0.27	5.41 ± 0.32	4.97 ± 0.42
15h	2.37 ± 0.13	3.31 ± 0.45	4.44 ± 0.37	5.21 ± 0.30	4.54 ± 0.27
15i	2.57 ± 0.36	4.39 ± 0.28	4.94 ± 0.47	5.47 ± 0.22	5.02 ± 0.16

Table 3
In vitro COX % inhibition studies.

Compound	% COX inhibition[a]		SI
	COX-1	COX-2	
15a	15.26	24.81	1.62
15b	28.21	55.10	1.95
15c	**42.26**	**63.23**	**1.49**
15d	26.89	40.83	1.52
15e	32.27	35.36	1.09
15f	**25.69**	**56.31**	**2.19**
15g	17.89	32.38	1.81
15h	49.18	27.88	0.57
15i	36.44	33.81	0.93
Indomethacin[b]	36.40	29.20	0.80
Diclofenac[c]	90.64	48.58	0.53

The enzyme inhibition for COX was calculated at 10 μM concentration for each compound.
SI (Selectivity index) = COX-1 IC_{50}/COX-2 IC_{50}.
[a] % inhibition is represented as mean value of two determinations (deviation less than is < 10%).

[b] The results are taken from reference [36]. [c]The results are taken from reference [37] at 10 μg/mL.

3.4. Antioxidant activity

The synthesized compounds exhibited the potential to scavenge free radicals in varying capacities in the DPPH assay. Activity was influenced by substitutions on aryl ring coupled to the oxadiazole/pyrazole nucleus. Compounds with halogens and methoxy group, emerged as better antioxidants amongst all the compounds. This superiority may be due to the presence of electron cloud on the aryl rings which can easily donate electron to DPPH. The free-radical scavenging activity of the synthesized compounds, which lack methoxy group is attributable to the presence of the oxadiazole nucleus itself. Donation of hydrogen leaves the

compounds in their radical form and their structure gets stabilized owing to electronic conjugation, thus favoring the reaction to occur. IC50 of the synthesized derivatives was also calculated and compounds 15c, 15e and 15f were found to be the most potent antioxidant agents, with IC_{50} (1.55, 2.48 and 2.51 μg/mL) comparable to ascorbic acid (1.18 μg/mL) (Table 4).

3.5. SAR studies

Careful inspection of correlation between the structures of the various synthesized molecules and the observed anti-inflammatory, analgesic and antioxidant activity showed a relationship between the varied substituents on the oxazole/pyrazole ring and the biological activity. However, the first and foremost conclusion drawn from the SAR observations was that the substitution on the 2nd position of indole nucleus decreased both the anti-inflammatory and analgesic activity of the synthesized compounds. Moreover, in case of anti-inflammatory profile, the compounds such as 15c, 15d, 15e and 15f with electron-withdrawing substituents on the aryl ring coupled to oxazole nucleus showed improved activity. While, unsubstituted/benzylated derivatives along with compounds having electron-donating substituents on the aryl ring coupled to oxazole nucleus showed decreased anti-inflammatory activity. In case of analgesic activity, a similar structure-activity profile was observed, with compounds having electron-withdrawing substituents showed better activity over unsubstituted or electron-donating group containing compounds. Overall, limited SAR derived from the developed compounds highlighted the significance of electron-withdrawing group as beneficial features for anti-inflammatory and analgesic activity.

3.6. Computational study

Considering the designing of the molecules which involves incorporating different pharmacophoric substructures present in well-established anti-inflammatory agents acting on different molecular targets [38], we utilized a detailed molecular docking analysis to understand the mechanism of action of these anti-inflammatory agents. All four prominent targets (COX-1, COX-2, LOX-5 and LOX-15) were therefore deliberated in this analysis against all 12 molecules. The docking protocol was validated by re-docking the co-crystallized ligand within the catalytic domain of specific selected target protein. It was observed that the re-docked pose of co-crystallized ligand retained the binding conformation to the co-crystallized pose with the RMSD value of < 1 Å. To identify the anti-inflammatory mechanism of the designed molecules, key interactions reported in previous studies as essential for the inhibition of the selected target were considered along with the obtained docking score for each hit.

The collected data indicated that in the case of COX-1, none of the analogs maintained the key H-bond interactions in the catalytic domain as observed in the reported COX-1 inhibitors. However, most of them did maintain crucial π-π interaction with Tyr385 (Table 5) and showed good estimated interaction energies (based on Glide docking scores) for the docked poses, with docking score ranging from −10.32 to −9.54 Kcal/mol. Nevertheless, failure to form crucial H-bonds suggests that mechanistically, these molecules do act via COX-1 inhibition. Against COX-2, conversely, these molecules, when optimally docked, maintained the required key H-bond interactions with Met522, and/or Ser530, along with other crucial interactions and accordingly showed excellent docking scores ranging from −11.12 to −6.65 Kcal/mol. One crucial information obtained during molecular docking analysis was that out of the 12 molecules, only 9 molecules belonging to indole-oxadiazole scaffold could bind to catalytic domain of COXs, while remaining 3 molecules belonging to indole-pyrazole scaffold were sterically unfavorable to occupy the binding pocket in both COX-1 and COX-2. Thus, each of these 9 indole-oxadiazole analogs studied are predicted to undergo preferable and stronger binding interactions with COX-2 over COX-1 binding domain, while the 3 molecules belonging to indole-pyrazole scaffold are not expected to act via any of the COX isoforms.

Extending the analysis to LOXs, the docking analysis with LOX-5 revealed that most of the compounds bind with the catalytic domain

Table 4
Antioxidant activity of compounds (**9a-c), (15a-i**).

Compd. Code	Absorbance	Absorbance at 517 nm (% Reduction in absorbance)					IC_{50} (μg/mL)
		2 μg/mL	4 μg/mL	6 μg/mL	8 μg/mL	10 μg/mL	
Control	$Abs_{control}$	0.689	0.689	0.689	0.689	0.689	–
Ascorbic acid	Abs_{sample}	0.365 (47.02)	0.289 (58.05)	0.218 (68.35)	0.189 (72.56)	0.114 (83.45)	1.18
9a	Abs_{sample}	0.473 (31.34)	0.421 (38.89)	0.379 (44.99)	0.288 (58.02)	0.260 (62.26)	3.30
9b	Abs_{sample}	0.448 (34.97)	0.406 (41.07)	0.332 (51.81)	0.269 (60.95)	0.201 (70.82)	2.70
9c	Abs_{sample}	0.429 (37.73)	0.402 (41.65)	0.309 (55.15)	0.259 (64.40)	0.209 (69.66)	2.57
15a	Abs_{sample}	0.415 (39.76)	0.393 (42.96)	0.301 (56.31)	0.252 (63.42)	0.211 (69.37)	2.45
15b	Abs_{sample}	0.469 (31.93)	0.388 (43.68)	0.345 (49.92)	0.285 (58.63)	0.239 (65.31)	3.01
15c	**Abs_{sample}**	**0.401 (41.79)**	**0.309 (55.15)**	**0.239 (65.31)**	**0.211 (69.37)**	**0.197 (71.40)**	**1.55**
15d	Abs_{sample}	0.404 (41.36)	0.389 (43.54)	0.340 (50.65)	0.265 (61.53)	0.202 (70.68)	2.53
15e	Abs_{sample}	0.439 (36.28)	0.359 (47.89)	0.311 (54.86)	0.261 (62.11)	0.209 (69.66)	2.48
15f	Abs_{sample}	0.429 (37.73)	0.379 (44.99)	0.329 (52.24)	0.241 (65.02)	0.201 (70.82)	2.51
15g	Abs_{sample}	0.439 (36.28)	0.383 (44.41)	0.307 (55.44)	0.247 (64.15)	0.219 (68.21)	2.55
15h	Abs_{sample}	0.481 (30.18)	0.373 (45.86)	0.334 (51.52)	0.283 (58.92)	0.245 (64.44)	2.97
15i	Abs_{sample}	0.449 (34.83)	0.393 (42.96)	0.319 (53.70)	0.231 (66.47)	0.203 (70.53)	2.61

% Reduction in absorbance = $(Abs_{control} - Abs_{test})/Abs_{control} \times 100$.
The inhibitory concentration (IC_{50}) value, representing the concentration required to exhibit 50% antioxidant activity. IC_{50} values were calculated by linear regression of plots where the abscissa represented the concentration of the compounds (μg/ml) and the ordinate, the average percentage of antioxidant activity.

Table 5
Results of molecular docking analysis for the indole functionalized pyrazoles/oxadiazoles.

S. No.	Compound ID	COX-1 (1PGF)		COX-2 (6COX)		LOX-5 (3 V99)		LOX-15 (1IK3)	
		Docking Score	H-bond	Docking score	H-bond	Docking score	H-bond	Docking core	H-bond
	9a		–	–	–	−4.725	Gln557, Gln363	–	–
	9b	–	–	–	–	−4.69	–	–	–
	9c	–	–	–	–	−5.857	–	–	–
	15a	–	–	−8.983	–	−5.153	Leu607, Fe701	−8.01	Hie513, Gln514, His518
	15b	−9.841	–	−9.826	Met522	−4.289	Gln363, Fe701	−5.001	Hie513
	15c	**−9.965**	**–**	**−11.126**	**Met522**	**−3.924**	Fe701	**−7.67**	Gln514, His518
	15d	−10.296	–	−6.652	–	−5.081	Leu607, Fe701	−7.279	His518
	15e	−9.818	–	−8.649	Phe518	−3.504	Gln363, Fe701, Phe610	−7.54	Gln514, Arg726
	15f	**−9.546**	**–**	**−8.497**	**Gln192, Leu352**	**−5.344**	Asn554	**−7.088**	Hie513
	15g	−10.17	–	−8.58	–	−6.039	Asn554, Tyr558	−6.457	–
	15h	−9.65	–	−8.327	Ser530	−4.157	Ala606	−6.513	Hie513, Gln514,
	15i	−10.32	–	−8.27	Ser530	−5.534	Val671	−5.346	Hie513

interacting with Fe^{2+} ion present as the co-factor. Importantly, the 3 molecules belonging to indole-pyrazole scaffold bound well to the catalytic site following a similar pose to the indole-oxadiazole analogs. Careful inspection disclosed that the nitrogen atoms present in oxadiazoles/pyrazoles were involved in chelating/interacting with the Fe. Overall, the molecules formed the key H-bond interactions with Gln363, Asn554 and Leu607 and showed good estimated interaction energies (based on Glide docking scores) for the docked poses, with docking score ranging from −6.03 to −3.50 Kcal/mol. Further, the docking analysis with LOX-15 revealed that most of the molecules make H-bond interaction with the histidine residues chelating with the co-factor. Also, some of the molecules formed the crucial H-bond interaction with Gln514 and showed good binding score (Glide score) ranging from −8.01 to −5.00 Kcal/mol. It is also worth mentioning that although many compounds showed better and preferable binding towards LOX-15 over LOX-5, the 3 molecules belonging to indole-pyrazole scaffold were again sterically unfavorable to occupy the binding pocket in LOX-15 and therefore can only be expected to act via LOX-5 as an anti-inflammatory agent. The detailed results of docking scores for each of the indole-oxadiazole analogs interacting with each of the anti-inflammatory targets are summarized in Table 5, and the 3D interaction diagrams of top hits with all four targets are shown in Fig. 2.

Finally, in order to assess the drug-like characteristics of these compounds, various physicochemical parameters of were evaluated [39]. Almost all the indole-oxadiazole based compounds showed good drug-like properties and follow Lipinski's rule of five, while indole-pyrazole violated one of the lipinski's rules (Table 6). The logP value of most of the compounds was found to be less than five and hydrogen bond donor and acceptor atoms are also less than five. Except a few, all the compounds showed 100% human oral absorption in Qikprop studies. The QP PCaco values were also in the optimum range and hence these compounds are expected to possess optimum cell membrane permeability. Thus, it can be concluded that most of the compounds have an optimum drug-like profile and can be developed as potential drug molecule.

4. Conclusion

In summary, 12 molecules pertaining to indole-oxadiazole and indole-pyrazole scaffolds were designed, synthesized and evaluated for their in-vivo anti-inflammatory, analgesic and anti-oxidant activities. To our delight, compounds belonging indole-oxadiazole scaffold demonstrated moderate to excellent anti-inflammatory activities in vivo, especially compounds 15c and 15f presented more promising and comprehensive NSAID-like profile in carrageenan-induced paw edema and tail flick experiments, in comparison to FDA-approved NSAID, Diclofenac and Indomethacin. After 1 h interval in *in vivo* anti-inflammatory studies, compound 15b showed maximum % inhibition amongst all compound in paw edema, however after 4 h it was found slightly less active which could be attributed to its metabolic liability. 15b is having unsubstituted aryl ring which could be more prone to metabolism and probably, therefore it is showing lower activity after 4 h. While, 15g although has good SI but still shows low inhibitory potential against COX-2 and probably therefore it is showing lower inhibitory potential in animal study. Further, exhaustive structure-based in-silico analysis disclosed that one class of molecules i.e., indole-oxadiazole derivatives may act by selectively inhibiting COX-2, while another class of molecules i.e., indole-pyrazole derivatives may act by blocking LOX-5. Overall, the results suggested that two compounds, 15c and 15f, can be further explored and developed as potent anti-inflammatory agents.

5. Experimental

5.1. Chemistry

The chemicals were purchased from Sigma-Aldrich, SRL and Avra and were used further without procurement. The solvents used in reactions were either dried or freshly distilled as per requirements and procedures. The progress of reactions was monitored using pre-coated silica TLC plates (Merck Silica-gel F254) using different mobile phases like hexane-ethyl acetate or chloroform-methanol for TLC development. The developed TLCs were visualized either under UV light at wavelengths of 254 nm and 360 nm or in iodine chamber. The melting points of synthesized compounds were recorded using Veego melting point apparatus and are uncorrected. ^{1}H NMR and ^{13}C NMR spectra were recorded on Bruker Advance II instrument at 400 MHz frequency, in $CDCl_3$ or DMSO and TMS ($\delta = 0$) as an internal standard at PU (Punjab University), Chandigarh. Chemical shifts have been expressed in δ values downfield from TMS. The multiplicity of NMR signals is designated as s (singlet), d (doublet), t (triplet), q (quartet), m (multiplet) and bs (broad singlet). Coupling constant (J) values are reported in hertz. IR spectra were recorded on Thermofischer FT-IR spectrophotometer using KBr pellets at ISF College of Pharmacy Moga.

5.1.1. General procedure for the preparation of hydrazone (3)

A mixture of acetophenone (5 g, 41.61 mmol, **1**) and phenylhydrazine (5 g, 46.23 mmol, **2**) were dissolved in ethanol (10 mL), taken in a well dried round bottom flask and 5–7 drops of glacial acetic acid was added into the reaction mixture. Then reaction mixture was stirred for 1–2 hrs at room temperature. The reaction progress was monitored by TLC. After completion of reaction, ethanol (4 mL) was added to the

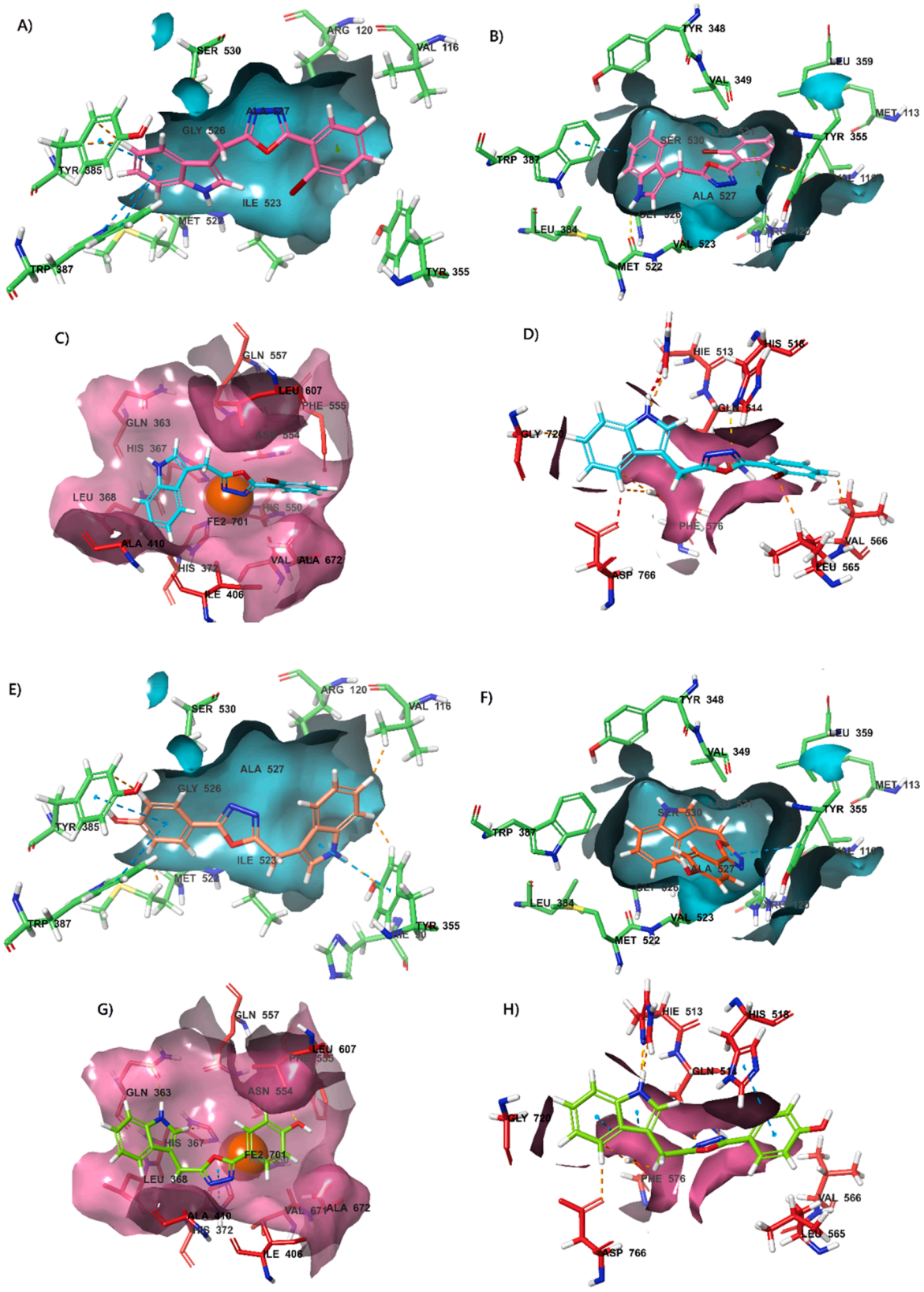

Fig. 2. 3-D interaction diagrams for the indole functionalized pyrazoles/oxadiazoles within the binding cavity of target enzymes a) 15c in COX-1b) 15c in COX-2c) 15c in LOX-5 d) 15c in LOX-15 e) 15f in COX-1f) 15f in COX-2 g) 15f in LOX-5 h) 15f in LOX-15.

Table 6
Physicochemical properties of the indole functionalized pyrazoles/oxadiazoles.

S. No.	Compound ID	Mol. MW	QP logPo/w	HB donor	HB acceptor	QP PCaco	QP logKhsa	Percent Oral Absorption	Rule of Five
1.	9a	379.46	5.688	1	3.5	3003.737	1.256	100	1
2.	9b	458.356	6.265	1	3.5	2998.352	1.402	100	1
3.	9c	413.521	7.868	1	1	6482.755	2.072	100	1
4.	15a	289.336	4.248	1	2.5	1720.586	0.619	100	0
5.	15b	275.309	3.742	1	2.5	1536.841	0.503	100	0
6.	15c	354.205	4.291	1	2.5	1840.676	0.627	100	0
7.	15d	309.754	4.237	1	2.5	1536.17	0.622	100	0
8.	15e	320.307	3.049	1	3.5	182.956	0.467	85.289	0
9.	15f	291.309	2.968	2	3.25	465.831	0.307	92.079	0
10.	15g	305.335	3.838	1	3.25	1568.368	0.52	100	0
11.	15h	290.324	2.754	2.5	3.5	399.854	0.238	89.638	0
12.	15i	305.335	3.852	1	3.25	1559.614	0.523	100	0

reaction mixture. The precipitated solid was then filtered, washed with cold hexane and dried to afford the acetophenone phenylhydazone (**3**) in good yield.

5.1.2. General procedure for the preparation of 2-Phenylindole (4)

Compound (**3**) (2.5 g, 11.90 mmol) and 10 g of polyphosphoric acid was heated for 1–2 hrs with continuous stirring. The reaction progress was monitored by TLC. After completion of reaction, 160 mL of cold water was added with well stirring. Precipitated solid was filtered under the vacuum, washed with 2–3 times of cold water and cold ethanol, dried to afford the 2-phenyl indole (**4**) in good yield.

5.1.3. General procedure for the preparation of 2-Phenylindole-3-carboxaldehyde (5)

Compound **4** (5.5 mmol, 1 eq) was added to the Vilsmeier-haack reagent prepared by the addition of $POCl_3$ (3.8 eq) in DMF (5.1 mmol of 4) at 0 °C. The mixture was stirred at 0 °C for 2 hrs to ensure the complete consumption of starting material by TLC monitoring. Then reaction was quenched slowly by adding ice and neutralized the reaction mixture by adding the 37% of NaOH solution. The resulting precipitate was filtered and dried to afford the 2-Phenylindole-3-carboxaldehyde (**5**) in good yield.

*5.1.4. **General procedure for the synthesis of Chalcone derivatives** (7)*

A mixture of 2-Phenylindole-3-carboxaldehyde (1 g, 4.51 mmol, **5**), acetophenone (0.5 mL, 4.51 mmol, **6**) and piperidine (1.8 mL) was taken in a well-dried round bottom flask and heated for 2–4 hrs, then ethanol (7 mL), glacial acetic acid and water (1:1) were added to resulting red solution until first appearance cloudiness. The progress of the reaction is monitored by TLC. The resulting product was filtered off and washed with water, dried to afford the desired product (**7**).

5.1.5. General procedure for the synthesis of pyrazoline derivatives (9a-c)

A mixture of Chalcone (500 mg, 1.54 mmol, **7a-b**), hydrazine hydrate (2.62 mmol, 1.7 eq, **8**) or phenylhydrazine (3.09 mmol, 2 eq, **8a**) and glacial acetic acid (6 mL) were refluxed for 5–7 hrs continuously. The reaction progress was monitored by TLC continuously using solvent system 30% ethyl acetate and hexane (3:7). On completion of the reaction (TLC monitoring) the resulting solution was cooled and neutralized with 20% KOH solution. After adding the crushed ice into resulting solution then precipitate was formed, filtered off, washed with cold water and dried to afford the final product in good yield.

*5.1.5.1. 1-(3-phenyl-5-(2-phenyl-1H-indol-3-yl)-4,5-dihydro-1H-pyrazol-1-yl)ethanone **(9a)**.* Light brown solid, **Yield:** 54%, **mp:** 190–192 °C, **Rf** 0.32, **IR** (KBr) νmax (cm^{-1}): 3444 (N—H stretching), 3049 (aromatic C—H stretching), 2350 (C═N stretching), 1620 (C═O), 1447 (C═C), 1209 (C—N). **^{1}H NMR** (500 MHz, DMSO-d_6) δ(ppm): 8.43 (s, 1H, NH), 7.85 (d, 1H, J = 8 Hz, Indole-C4), 7.56 (d, 1H, J = 8 Hz, Indole-C7), 7.47–7.39 (10*H*, m, Ar-H),7.28 (dt, 1H, J_1 = 8 Hz, J_2 = 4 Hz, Indole-C6), 7.21 (dt, 1H, J_1 = 8 Hz, J_2 = 4 Hz, Indole-C5), 6.78 (t, 1H, J = 4 Hz, Pyrazoline), 3.87 (dd, 1H, J_1 = 4 Hz, J_2 = 12 Hz, Pyrazoline-H), 3.45 (dd, 1H, J_1 = 4 Hz, J_2 = 12 Hz, Pyrazoline-H), 2.27 (s, 3H, CH_3); **^{13}C NMR** (175 MHz, DMSO-d_6) δ(ppm): 169.37, 151.49, 138.78, 135.34, 132.23, 131.97, 129.65, 128.32, 128.11, 127.98, 127.87, 126. 85, 125.96, 124.13, 120.93, 120.04, 115.91, 110.86, 55.33, 40.45, 21.96; **MS: *m/z* [M]** $^+$ for $C_{25}H_{21}N_3O$, calculated 379.16; observed: 379.

*5.1.5.2. 1-(3-(4-bromophenyl)-5-(2-phenyl-1H-indol-3-yl)-4,5-dihydro-1H-pyrazol-1-yl)ethan-1-one **(9b)**.* Dark brown solid, **Yield:** 52%, **mp:** 188–190 °C**, Rf** 0.20, **IR** (KBr) νmax (cm^{-1}): 3444 (N—H stretching), 3050 (aromatic C—H stretching), 2305(C═N stretching), 1638 (C═O), 1470 (C═C), 1209 (C—N), 665 (C-Br). **^{1}H NMR** (500 MHz, DMSO-d_6) δ(ppm): 8.52 (s, 1H, NH), 7.85 (d, 1H, J = 8 Hz, Indole-C4), 7.51 (d, 1H, J = 8 Hz, Indole-C7), 7.76 (d, 2H, J = 8 Hz, Ar-H attached to pyrazoline), 7.62 (d, 2H, J = 8 Hz, Ar-H attached to pyrazoline), 7.49–7.41 (5H, m, Ar-H), 7.31 (dt, 1H, J_1 = 8 Hz, J_2 = 4 Hz, Indole-C6), 7.23 (dt, 1H, J_1 = 8 Hz, J_2 = 4 Hz, Indole-C5), 6.75 (t, 1H, J = 4 Hz, Pyrazoline), 3.79 (dd, 1H, J_1 = 4 Hz, J_2 = 12 Hz, Pyrazoline-H), 3.38 (dd, 1H, J_1 = 4 Hz, J_2 = 12 Hz, Pyrazoline-H), 2.26 (s, 3H, CH_3); **^{13}C NMR** (175 MHz, DMSO-d_6) δ(ppm): 169.42, 151.56, 138.91, 135.46, 132.41, 132.16, 129.83, 128.51, 128.28, 128.09, 128.01, 126.99, 126.16, 124.28, 121.07, 120.21, 116.03, 110.97, 55.52, 40.57, 22.12. **MS: *m/z* [M]** $^+$ for $C_{25}H_{20}BrN_3O$, calculated 457.07; observed: 457.

*5.1.5.3. 3-(1,3-diphenyl-4,5-dihydro-1H-pyrazol-5-yl)-2-phenyl-1H-indole **(9c)**.* Brown solid, **Yield:** 65%, **mp:** 195–197 °C**, Rf** 0.43, **IR** (KBr) νmax (cm^{-1}): 3342 (N—H stretching), 3050 (aromatic C—H stretching), 2316 (C═N stretching), 1565 (C═C), 1230 (C—N). **^{1}H NMR** (500 MHz, DMSO-d_6) δ(ppm): 8.45 (s, 1H, NH), 7.83 (d, 1H, J = 8 Hz, Indole-C4), 7.54 (d, 1H, J = 8 Hz, Indole-C7), 7.67 (d, 2H, J = 8 Hz, Ar-H), 7.54–7.39 (m, 9H, Ar-H), 7.31–7.16 (m, 4H, Ar-H, Indole), 6.99–6.96 (m, 2H, Ar-H), 6.23 (t, 1H, J = 4 Hz, Pyrazoline), 3.83 (dd, 1H, J_1 = 4 Hz, J_2 = 12 Hz, Pyrazoline-H), 3.47 (dd, 1H, J_1 = 4 Hz, J_2 = 12 Hz, Pyrazoline-H); **^{13}C NMR** (175 MHz, DMSO-d_6) δ(ppm): 154.21, 145.19, 140.89, 137.11, 133.98, 132.87, 131.54, 129.13, 128.82, 128.11, 128.08, 127.46, 125.39, 122.03, 121.79, 121.37, 117.84, 115.75, 112.18, 60.18, 40.88; **MS: *m/z* [M]** $^+$ for $C_{29}H_{23}N_3$, calculated 413.19; observed: 413.

5.1.6. General procedure for the synthesis of Indole ester (11)

Compound **10,** Indole-3-acetic acid (5 g, 28.54 mmol), was taken in a well dried round bottom flask containing ethanol (15 mL) and 10–12 drops of conc. sulfuric acid were added. The contents were refluxed for 2–3 hrs. The reaction progress was monitored by TLC. After completion, the reaction mixture was cooled at room temperature and sodium metasulphite was added to consume the excess acid. Then mixture was filtered off and collected the filtrate. The excess solvent was evaporated from the mixture to afford indole-3-acetic ester (**11**) in good yield and used for further reaction without purification.

5.1.7. General procedure for the preparation of Indole-3-acetic hydrazide (13)

A mixture of Indole-3-acetic ester (5 g, 24.60 mmol, **11**) and hydrazine hydrate (147.60 mmol, 6 eq, **12**) was taken in a well-dried round bottom flask and refluxed for 2–3 hrs. The reaction progress was monitored by TLC continuously using solvent system 30% ethyl acetate and hexane (3:7). On completion of the reaction (TLC monitoring) the resulting solution was cooled at RT and excess solvent was removed by Rota evaporator. The resulting mixture was kept in the refrigerator for 3–4 hrs and then a crystal of ice was added and it initiated the crystallization of our product. The pure crystals of required product were separated, dried to afford the Indole-3-acetic hydrazide (**13**) in high yield and used for the further reaction.

5.1.8. General procedure for the preparation of oxadiazole derivatives (15a-i)

A mixture of Indole-3-acetic hydrazide (1 g, 5.28 mmol, **13**), different aromatic acids (5.28 mmol, 1 eq, **13**) and phosphorus oxychloride (5 mL) were taken in a well-dried round bottom flask and heated for 5–6 hrs at 60 °C. The reaction progress was monitored by TLC continuously using solvent system 20% acetone and hexane (2:8). On completion of the reaction (TLC monitoring) the resulting mixture was cooled at room temperature. The resulting mixture was neutralized by adding the aqueous solution of sodium bicarbonate and mixture was cooled in refrigerator to form the precipitate of required product. The precipitate was filtered off, washed with cold water, dried and recrystallized from aqueous ethanol to afford the final product in good yield.

*5.1.8.1. 2-((1H-indol-3-yl)methyl)-5-benzyl-1,3,4-oxadiazole **(15a)**.* Dark brown solid, **Yield:** 54%, **mp:** 163–165 °C**, Rf** 0.32, **IR** (KBr) νmax (cm-^{1}): 3280 (N—H stretching), 3053 (aromatic C—H stretching), 2950 (aliphatic C—H stretching), 2357 (C═N), 1574 (aromatic C═C), 1358 (C—N stretching), 1235 (C—O). **^{1}H NMR** (500 MHz, DMSO-d_6) δ(ppm): 8.34 (s, 1H, NH), 7.79 (s, 1H, indole-*C*2), 7.61 (d, 1H, J = 8 Hz, Indole-C4), 7.38 (d, 1H, J = 8 Hz, Indole-C7), 7.30–7.25 (m, 4H, Ar-H), 7.21–7.16 (m, 3H, Ar-H, indole), 4.85 (s, 2H, CH_2), 4.03 (s, 2H, CH_2), **^{13}C NMR** (175 MHz, DMSO-d_6) δ(ppm): 166.38, 163.95, 136.23, 134.52, 127.87, 127.53, 127.34, 126.33, 121.67, 119.32, 119.10, 110.97, 108.45, 33.54, 26.26. **MS: *m/z* [M]$^+$ for $C_{18}H_{15}N_3O$**, calculated 289.12; observed: 289.

*5.1.8.2. 2-((1H-indol-3-yl)methyl)-5-phenyl-1,3,4-oxadiazole **(15b)**.* Blackish brown solid, **Yield:** 58%, **mp:** 172–174 °C**, Rf** 0.20, **IR** (KBr) νmax (cm-^{1}): 3310 (N—H stretching), 3057 (aromatic C—H stretching), 2952 (aliphatic C—H stretching), 2316 (C═N), 1574 (aromatic C═C), 1340 (C—N stretching), 1220 (C—O). **^{1}H NMR** (500 MHz, DMSO-d_6) δ(ppm): 8.28 (s, 1H, NH), 7.74 (s, 1H, indole-*C*2), 7.57 (d, 1H, J = 8 Hz, Indole-C4), 7.35 (d, 1H, J = 8 Hz, Indole-C7), 7.59–7.51 (m, 3H, Ar-H), 7.41–7.35 (m, 2H, Ar-H), 7.27 (dd, 1H, J_1 = 8 Hz, J_2 = 4 Hz, Indole-C6), 7.18 (dd, 1H, J_1 = 8 Hz, J_2 = 4 Hz, Indole-C5), 4.82 (s, 2H, CH_2), **^{13}C NMR** (175 MHz, DMSO-d_6) δ(ppm): 165.99, 163.78, 136.11, 132.82, 128.79, 127.28, 127.02, 125.34, 123.23, 121.78, 120.76, 119.12, 110.79, 107.82, 26.26. **MS: *m/z* [M]$^+$ for $C_{17}H_{13}N_3O$,** calculated 275.10; observed: 275.

*5.1.8.3. 2-((1H-indol-3-yl)methyl)-5-(2-bromophenyl)-1,3,4-oxadiazole **(15c)**.* Yellowish brown solid, **Yield:** 60%, **mp:** 198–200 °C**, Rf** 0.43, **IR** (KBr) νmax (cm-^{1}) νmax (cm-1): 3265 (N—H stretching), 3056 (aromatic C—H stretching), 2924 (aliphatic C—H stretching), 1574 (C═C), 1358 (C—N), 1235 (C—O), 670 (C-Br). **^{1}H NMR** (500 MHz, DMSO-d_6) δ(ppm): 8.29 (s, 1H, NH), 8.17 (s, 1H, Indole-*C*2), 7.83 (d, 1H, J = 8 Hz, Indole-C4), 7.70 (d, 1H, J = 8 Hz, Indole-C7), 7.68 (d, 1H, Ar-H, J = 8 Hz), 7.40–7.31 (m, 3H, Ar-H), 7.24–7.20 (m, 1H, Ar-H, indole), 7.14 (t, 1H, Ar-H, J = 8 Hz), 4.45 (s, 2H, CH_2), **^{13}C NMR** (175 MHz, DMSO-d_6) δ(ppm): 166.31, 163.90, 136.18, 134.44, 132.36, 131.60, 127.53, 126.81, 125.40, 123.20, 122.51, 121.59, 119.94, 118.81, 111.35, 108.17, 22.26. **MS: *m/z* [M]$^+$ for $C_{17}H_{12}BrN_3O$**, calculated 353.01; observed: 353.

*5.1.8.4. 2-((1H-indol-3-yl)methyl)-5-(4-chlorophenyl)-1,3,4-oxadiazole **(15d)**.* Brown solid, **Yield:** 70%, **mp:** 180–182 °C**, Rf** 0.56, **IR** (KBr) νmax (cm-^{1}): 3447 (N—H stretching), 3226 (aromatic C—H stretching), 2991 (aliphatic C—H stretching), 2391 (C═N), 1653 (aromatic C═C), 1289 (C—N stretching). 1135 (C—O), 780 (C-Cl). **^{1}NMR** (500 MHz, DMSO-d_6) δ(ppm): 8.43 (s, 1H, NH), 8.19 (s, 1H, Indole-*C*2), 8.03 (d, 2H, J = 8 Hz, Ar-H), 7.85 (d, 1H, J = 8 Hz, Indole-C4), 7.74 (d, 1H, J = 8 Hz, Indole-C7), 7.48 (d, 2H, J = 8 Hz, Ar-H), 7.21–7.17 (m, 2H, Indole-C5 and C6), 4.47 (s, 2H, CH_2), **^{13}C NMR** (175 MHz, DMSO-d_6) δ(ppm): 165.87, 163.38, 136.18, 134.01, 133.93, 129.43, 128.05, 126.27, 124.51, 123.70, 121.65, 120.43, 119.44, 111.45, 107.86, 23.34. **MS: *m/z* [M]$^+$ for $C_{17}H_{12}ClN_3O$**, calculated 309.06; observed: 309.

*5.1.8.5. 2-((1H-indol-3-yl)methyl)-5-(4-nitrophenyl)-1,3,4-oxadiazole **(15e)**.* Brown solid, **Yield:** 60%, **mp:** 198–200 °C**, Rf** 0.7, **IR** (KBr) νmax (cm-^{1}): 3404 (N—H stretching), 3108 (aromatic C—H stretching), 2849 (aliphatic C—H stretching), 2316 (C═N), 1571 (aromatic C═C), 1518 and 1340 (N—O), 1190 (C—N stretching), 1030 (C—O). **^{1}NMR** (500 MHz, DMSO-d_6) δ(ppm): 8.47 (s, 1H, NH), 8.21 (m, 3H, Indole-*C*2, Ar-H), 8.14 (d, 2H, J = 8 Hz, Ar-H), 7.87 (d, 1H, J = 8 Hz, Indole-C4), 7.76 (d, 1H, J = 8 Hz, Indole-C7), 7.16 (dd, 1H, J_1 = 8 Hz, J_2 = 4 Hz, Indole-C6), 7.09 (dd, 1H, J_1 = 8 Hz, J_2 = 4 Hz, Indole-C5), 4.49 (s, 2H, CH_2), **^{13}C NMR** (175 MHz, DMSO-d_6) δ(ppm): 165.97, 163.48, 148.73, 136.60, 129.65, 127.47, 126.68, 125.29, 123.01, 122.35, 121.39, 111.23, 108.06, 23.78. **MS: *m/z* [M]$^+$ for $C_{17}H_{12}N_4O_3$**, calculated 320.09; observed: 320.

*5.1.8.6. 4-(5-((1H-indol-3-yl)methyl)-1,3,4-oxadiazol-2-yl)phenol **(15f)**.* Dark brown solid, **Yield:** 75%, **mp:** 165–167 °C**, Rf** 0.8, **IR** (KBr) νmax (cm-^{1}): 3404 (O—H stretching), 3209 (N—H stretching), 3068 (aromatic C—H stretching), 2849 (aliphatic C—H stretching), 2348 (C═N), 1610 (aromatic C═C), 1085 (C—N stretching), 1030 (C—O). **^{1}NMR** (500 MHz, DMSO-d_6) δ(ppm): 11.06 (s, 1H, OH), 8.43 (s, 1H, NH), 7.79 (d, 1H, J = 8 Hz, Indole-C4), 7.58 (d, 1H, J = 8 Hz, Indole-C7), 7.46–7.24 (m, 3H, Ar-H), 7.09 (t, 1H, Ar-H, J = 8 Hz, Indole-C6), 7.01 (t, 1H, Ar-H, J = 8 Hz, Indole-C5), 6.91 (d, 2H, J = 8 Hz, Ar-H), 4.38 (s, 2H, CH2), **^{13}C NMR** (125 MHz, CDCl3): 165.05, 164.04, 160.53, 136.10, 128.09, 126.53, 123.97, 121.17, 118.62, 118.11, 116.00, 114.07, 111.48, 106.84, 21.43. **MS: *m/z* [M]$^+$ for $C_{17}H_{13}N_3O_2$**, calculated 291.10; observed: 291.

*5.1.8.7. 2-((1H-indol-3-yl)methyl)-5-(4-methoxyphenyl)-1,3,4-oxadiazole **(15g)**.* Yellowish brown solid, **Yield:** 80%, **mp:** 145–147 °C**, Rf** 0.8, **IR** (KBr) νmax (cm-^{1}): 3309 (N—H stretching), 3068 (aromatic C—H stretching), 2919 (aliphatic C—H stretching), 2316 (C═N), 1610 (aromatic C═C), 1176 (C—N stretching), 1130 (C—O). **^{1}NMR** (500 MHz, DMSO-d_6) δ(ppm): 8.45 (s, 1H, NH), 8.02 (s, 1H, Indole-*C*2), 7.87 (d, 2H, Ar-H, J = 8 Hz), 7.81 (d, 1H, J = 8 Hz, Indole-C4), 7.68 (d, 1H, J = 8 Hz, Indole-C7), 7.29 (dt, 1H, J_1 = 8 Hz, J_2 = 4 Hz, Indole-C6), 7.21 (dt, 1H, J_1 = 8 Hz, J_2 = 4 Hz, Indole-C5), 6.97 (d, 2H, Ar-H, J = 8 Hz), 4.49 (s, 2H, CH_2), 3.83 (s, 3H, OCH_3), **^{13}C NMR** (175 MHz, DMSO-d_6) δ(ppm): 166.52, 164.03, 163.07, 136.98, 127.04, 126.78, 123.97, 121.77, 120.52, 119.23, 118.83, 115.27, 112.02, 107.54, 54.33, 23.12. **MS: *m/z* [M]$^+$ for $C_{18}H_{15}N_3O_2$,** calculated 305.11; observed: 305.

*5.1.8.8. 4-(5-((1H-indol-3-yl)methyl)-1,3,4-oxadiazol-2-yl)aniline **(15h)**.* Light brown solid, **Yield:** 78%, **mp:** 193–195 °C**, Rf** 0.6, **IR** (KBr) νmax (cm-^{1}): 3354 (N—H stretching), 3056 (aromatic C—H stretching), 2926 (aliphatic C—H stretching), 2374 (C═N), 1631 (aromatic C═C), 1608 (N—H bending), 1246 (C—N stretching), 1090 (C—O). **^{1}NMR** (500 MHz, DMSO-d_6) δ(ppm): 8.47 (s, 1H, NH), 8.03 (s, 1H, Indole-*C*2),

7.83 (d, 1H, $J = 8$ Hz, Indole-C4), 7.77 (d, 2H, Ar-H, $J = 8$ Hz), 7.70 (d, 1H, $J = 8$ Hz, Indole-C7), 7.31 (dt, 1H, $J_1 = 8$ Hz, $J_2 = 4$ Hz, Indole-C6), 7.23 (dt, 1H, $J_1 = 8$ Hz, $J_2 = 4$ Hz, Indole-C5), 6.82 (d, 2H, Ar-H, $J = 8$ Hz), 4.53 (s, 2H, CH_2), 4.48 (bs, 2H, Ar-NH_2), **^{13}C NMR** (175 MHz, DMSO-d_6) δ(ppm): 165.87, 163.38, 151.37, 135.76, 127.08, 126.31, 123.35, 121.48, 120.51, 119.23, 118.67, 115.97, 111.53, 107.98, 24.76. **MS: *m/z* [M]$^+$ for $C_{17}H_{14}N_4O$**, calculated 290.11; observed: 290.

*5.1.8.9. 2-((1H-indol-3-yl)methyl)-5-(3-methoxyphenyl)-1,3,4-oxadiazole **(15i)**.* Brown solid, **Yield:** 65%, **mp:** 178–180 °C, **Rf** 0.5, **IR** (KBr) νmax (cm^{-1}): 3301 (N—H stretching), 3045 (aromatic C—H stretching), 2943 (aliphatic C—H stretching), 2316 (C═N), 1531 (aromatic C═C), 1608, 1276 (C—N stretching), 1190 (C—O). **^{1}NMR** (500 MHz, DMSO-d_6) δ(ppm): 8.28 (s, 1H, NH), 8.17 (s, 1H, Indole-*C*2), 7.85 (d, 1H, $J = 8$ Hz, Indole-C4), 7.75 (d, 1H, $J = 8$ Hz, Indole-C7), 7.70 (d, 1H, Ar-H, $J = 8$ Hz), 7.41–7.35 (m, 3H, indole-C7, Ar-H), 7.34 (dt, 1H, $J_1 = 8$ Hz, $J_2 = 4$ Hz, Indole-C6), 7.26 (dt, 1H, $J_1 = 8$ Hz, $J_2 = 4$ Hz, Indole-C5), 6.98 (d, 1H, Ar-H, $J = 8$ Hz), 4.48 (s, 2H, CH_2), 3.81 (s, 3H, OCH_3), **^{13}C NMR** (175 MHz, DMSO-d_6) δ(ppm): 165.46, 163.65, 162.87, 136.95, 129.48, 126.84, 125.78, 123.87, 121.65, 121.60, 120.70, 120.52, 118.95, 111.87, 111.75, 107.42, 56.13, 23.34. **MS: *m/z* [M]$^+$ for $C_{18}H_{15}N_3O_2$,** calculated 305.11; observed: 305.

5.2. In-vivo studies

5.2.1. Anti-inflammatory activity

The synthesized compounds were evaluated for their anti-inflammatory activity t using carrageenan-induced paw oedema method in Wistar rats of either sex, weighing 160–180 g (n = 6) [40]. Briefly, the rats were administered suspension of test compounds (50 mg/kg, orally) in PEG 400, 30 min before carrageenan injection (0.1 mL saline, containing 1% carrageenan). The rats of control group received the same volume of vehicle. Indomethacin was used as standard anti-inflammatory agents at concentrations of 5, 7.5 and 10 mg/kg. The volume of the paw was measured by a plethysmometer immediately after the injection. Subsequent readings of the volume of the same paw were recorded at 1, 2, 4 h intervals. The percent anti-inflammatory activity was calculated according to the following formula:

$$\text{Percentage inhibition of edema} = (1 - \text{Vt}/\text{Vc}) \times 100$$

Where, Vt and Vc are volumes of edema in drug treated and control groups, respectively.

5.2.2. Analgesic activity

The analgesic activity of synthesized compounds at a dose of 50 mg/kg was evaluated using tail flick method in Wistar rats of either sex, weighing 160–180 g (n = 6). The analgesic potential was measured by using Dynamic Plantar Aesthesiometer [41]. In this method, first the rats were habituated for two hours before performing the experiment to familiarize them. The mechanical threshold was measured by an electronic von Frey tip and calculated the force applied by withdrawal of paw. The test compounds were administered orally at mentioned dose while the Declofenac was used as standard drug at dose of 40 mg/kg. The tip of the tail was placed on heat source and basal reaction time to heat stimulus was noted. The tail was withdrawn by the animal and this was considered the endpoint [42]. The reaction time of tail was noted at interval of 30 min, 1, 2, 3 h intervals after dose administration. Each test was repeated five times at average cut off 20 *sec*. The maximum and minimum values are excluded, and the average of remained three values was used for mechanical threshold. The values are expressed as mean ± SD.

5.3. In-vitro COX inhibitory study

The synthesized compounds were screened for *in vitro* COX-1 and COX-2 inhibitory activities using COX inhibitor screening assay kit (Cayman chemical company) [43]. The compounds were screened at one concentration (10 μM) against ovine COX-1 and human COX-2 for determining inhibition and their selectivity as per protocol described by manufacturer. The inhibitors for COX-1/COX-2 were taken in 950 μL buffer (Co-solvated in DMSO) and added 10 μL heme followed by 10 μL of respective enzyme. For background inactivated enzyme was used in reaction. Reaction was initiated by adding 10 μL arachidonic acid and incubated at 37 °C for 2 min. The reaction was stopped by adding 50 μL HCl after which 100 μL of $SnCl_2$ was added which reduce PGH_2 initially formed to $PGF_2\alpha$. The amount of $PGF_2\alpha$ formed was determined in 96 well plate using ELISA reader at 406 nm wavelength. The results are expressed as percentage inhibition of respective enzymes at 10 μM concentration.

5.4. Antioxidant activity

The antioxidant activity of synthesized compounds was evaluated using DPPH (1,1-diphenyl-2-picrylhydrazyl) free radical scavenging assay with ascorbic acid as standard. DPPH solution was prepared by dissolving 0.1 mM DPPH in methanol and kept in dark for 2 h. After 2 h, 2 mL of this DPPH solution was taken, added 2 mL of different concentrations of test samples (2, 4, 6, 8 and 10 μg/mL) and mixed thoroughly. The resulting mixture was incubated for 30 min at room temperature and absorbance was recorded at wavelength of 517 nm [44,45]. The assay was performed in triplicate and values were expressed as mean ± standard deviation. The percentage of free radical scavenging activity was calculated by using following:

$$\text{Percentage scavenging} = (\text{A} - \text{B})/\text{A} \times 100$$

Where, A = absorbance of control (DPPH); B = absorbance of sample

5.5. In-Silico studies

Total 12 indole functionalized pyrazole and oxadiazole derivatives were sketched and cleaned by utilizing the *builder tool* option in the Schrödinger 2020–4 molecular modeling platform (Schrödinger Inc, USA). The molecules were optimized with OPLS3e force field [46] using the *Ligprep* module of *Schrödinger* at pH range of 7.0 ± 0.5. For the molecular docking analysis in different anti-inflammatory targets including COX-1, COX-2, LOX-5 and LOX-15, the co-crystallised structure 1PGF, 6COX, 3 V99 and 1IK3, respectively, were obtained from the Protein Data Bank (PDB; www.rcsb.org). These structures were chosen on the basis of their resolution and considering the co-crystallized ligands. *Protein Preparation Wizard* in the Schrödinger platform was used to add the hydrogen atoms and partial charges, and to check the bond orders. Water molecules in all the system were removed and energy was minimized using an OPLS3e force field. *Glide* module in Schrödinger, which is based on the OPLS3e force field, was used to perform the molecular docking analysis with high accuracy using the XP (extra precision) mode where further elimination of false positives is accomplished by more extensive sampling and advanced scoring, resulting in even higher enrichment. The position of glide grid was defined based on the co-crystallized ligands in the already prepared (both X-ray solved and homology modelled) proteins. Post-docking minimization was executed to optimize the ligand geometries [47]. Further, Qikprop module of Schrödinger was used to predict the drug-like and ADME properties of the compounds [48].

Declaration of Competing Interest

The authors declare that they have no known competing financial interests or personal relationships that could have appeared to influence the work reported in this paper.

Acknowledgements

The authors are also thankful to Mr. Praveen Garg, Chairman and Prof. (Dr) G. D. Gupta, Director cum Principal, ISF College of Pharmacy, Moga, Punjab for his continuous support and encouragement. PKS would like to thank TCSMT (University of Turku) for research funding.

References

[1] S.I. Grivennikov, F.R. Greten, M. Karin, Immunity, inflammation, and cancer, Cell 140 (2010) 883–899.
[2] S. Sharma, D. Kumar, G. Singh, V. Monga, B. Kumar, Recent advancements in the development of heterocyclic anti-inflammatory agents, Eur. J. Med. Chem. 112438 (2020).
[3] S. Steinmann, M. Schoedsack, F. Heinrich, P.C. Breda, A. Ochel, G. Tiegs, K. Neumann, Hepatic ILC2 activity is regulated by liver inflammation-induced cytokines and effector CD4+ T cells, Sci. Rep. 10 (1) (2020) 1–13.
[4] V. Menkin, Inflammation: a protective mechanism, Arch. Intern. Med. 48 (1931) 249–261.
[5] O. Takeuchi, S. Akira, Pattern recognition receptors and inflammation, Cell 140 (2010) 805–820.
[6] R. Medzhitov, Inflammation 2010: new adventures of an old flame, Cell 140 (2010) (2010) 771–776.
[7] O. Chertov, D. Yang, O.Z. Howard, J.J. Oppenheim, Leukocyte granule proteins mobilize innate host defenses and adaptive immune responses, Immunol. Rev. 177 (2000) 68–78.
[8] S.M. Opal, V.A. DePalo, Anti-inflammatory cytokines, Chest 117 (2000) 1162–1172.
[9] C.A. Feghali, T.M. Wright, Cytokines in acute and chronic inflammation, Front. Biosci. 2 (1997) d12–d26.
[10] G. Arango Duque, A. Descoteaux, Macrophage cytokines: involvement in immunity and infectious diseases, Front. Immunol. 5 (2014) 491.
[11] Y. Zhou, Y. Hong, H. Huang, Triptolide attenuates inflammatory response in membranous glomerulo-nephritis rat via downregulation of NF-κB signaling pathway, Kidney Blood Pressure Res. 41 (2016) 901–910.
[12] J.H. Fritz, S.E. Girardin, How Toll-like receptors and Nod-like receptors contribute to innate immunity in mammals, J. Endotoxin Res. 11 (2005) 390–394.
[13] V.S. Hanna, E.A.A. Hafez, Synopsis of arachidonic acid metabolism: A review, J. Adv. Res. 11 (2018) 23–32.
[14] Z. Ye, Y. Shen, K. Jin, J. Qiu, B. Hu, R.R. Jadhav, K. Sheth, C.M. Weyand, J. J. Goronzy, Arachidonic acid-regulated calcium signaling in T cells from patients with rheumatoid arthritis promotes synovial inflammation, Nat. Commun. 12 (1) (2021) 1–17.
[15] A. Gaddi, A.F. Cicero, E.J. Pedro, Clinical perspectives of anti-inflammatory therapy in the elderly: the lipoxigenase (LOX)/cycloxigenase (COX) inhibition concept, Arch. Gerontol. Geriatr. 38 (2004) 201–212.
[16] X. Gao, R. Zhu, J. Du, W. Zhang, W. Gao, L. Yang, Inhibition of LOX-1 prevents inflammation and photoreceptor cell death in retinal degeneration, Int. Immunopharmacol. 80 (2020), 106190.
[17] D.M. Poetker, D.D. Reh, A comprehensive review of the adverse effects of systemic corticosteroids, Otolaryngol. Clin. North Am. 43 (2010) 753–768.
[18] R.O. Day, G.G. Graham, Non-steroidal anti-inflammatory drugs (NSAIDs), BMJ 346 (2013), f3195.
[19] P. Chawla, S. Kalra, R. Kumar, R. Singh, S.K. Saraf, Novel 2-(substituted phenyl Imino)-5-benzylidene-4-thiazolidinones as possible non-ulcerogenic tri-action drug candidates: synthesis, characterization, biological evaluation And docking studies, Med. Chem. Res. 28 (3) (2019) 340–359.
[20] D. Kumar, S. Sharma, S. Kalra, G. Singh, V. Monga, B. Kumar, Medicinal Perspective of Indole Derivatives: Recent Developments and Structure-Activity Relationship Studies, Curr. Drug Targets 21 (9) (2020) 864–891.
[21] R.J. Flower, The development of COX2 inhibitors, Nat. Rev. Drug Discov. 2 (2003) 179–191.
[22] D.O. Stichtenoth, J.C. Frölich, The second generation of COX-2 inhibitors, Drugs 63 (2003) 33–45.
[23] B. Nehra, S. Rulhania, S. Jaiswal, B. Kumar, G. Singh, V. Monga, Recent advancements in the development of bioactive pyrazoline derivatives, Eur. J. Med. Chem. 112666 (2020).
[24] M. Arora, S. Choudhary, P.K. Singh, B. Sapra, O. Silakari, Structural investigation on the selective COX-2 inhibitors mediated cardiotoxicity: A review, Life Sci. 251 (2020), 117631.
[25] J. Kirchrath, K. Schrr, Cyclooxygenase-2 inhibition and side-effects of non-steroidal anti-inflammatory drugs in the gastrointestinal tract, Curr. Med. Chem. 7 (2000) 1121–1129.
[26] J. Martinez-Gonzalez, L. Badimon, Mechanisms underlying the cardiovascular effects of COX-inhibition: benefits and risks, Curr. Pharm. Design 13 (2007) 2215–2227.
[27] P. Rao, E.E. Knaus, Evolution of nonsteroidal anti-inflammatory drugs (NSAIDs): cyclooxygenase (COX) inhibition and beyond, J. Pharm. Pharm. Sci. 11 (2008) 81–110s.
[28] H.S. ElBordiny, M.M. El-Miligy, S.E. Kassab, H. Daabees, W.A.M. Ali, S.A.M. El-Hawash, Design, synthesis, biological evaluation and docking studies of new 3-(4, 5-dihydro-1H-pyrazol/isoxazol-5-yl)-2-phenyl-1H-indole derivatives as potent antioxidants and 15-lipoxygenase inhibitors, Eur. J. Med. Chem. 145 (2018) 594–605.
[29] J. Fort, Celecoxib, a COX-2–specific inhibitor: the clinical data, Am. J. Orthop. (Belle Mead, NJ) 28 (1999) 13-18.
[30] L. Gong, C.F. Thorn, M.M. Bertagnolli, T. Grosser, R.B. Altman, T.E. Klein, Celecoxib pathways: pharmacokinetics and pharmacodynamics, Pharmacogenet. Genomics 22 (2012) 310.
[31] J. Boström, A. Hogner, A. Llinàs, E. Wellner, A.T. Plowright, Oxadiazoles in medicinal chemistry, J. Med. Chem. 55 (2012) 1817–1830.
[32] A. Rathore, R. Sudhakar, M.J. Ahsan, A. Ali, N. Subbarao, S.S. Jadav, S. Umar, M. S. Yar, In vivo anti-inflammatory activity and docking study of newly synthesized benzimidazole derivatives bearing oxadiazole and morpholine rings, Bioorg. Chem. 70 (2017) 107–117.
[33] S.A. Khan, K. Saleem, Z. Khan, Synthesis, characterization and in vitro antibacterial activity of new steroidal thiazolo quinoxalines, Eur. J. Med. Chem. 42 (2007) 103–108.
[34] S. Wagle, A.V. Adhikari, N.S. Kumari, Synthesis of some new 2-(3-methyl-7-substituted-2-oxoquinoxalinyl)-5-(aryl)-1, 3, 4-oxadiazoles as potential non-steroidal anti-inflammatory and analgesic agents, Indian J. Chem. 47 (2008) 439–448.
[35] S.V. Bhandari, K.G. Bothara, M.K. Raut, A.A. Patil, A.P. Sarkate, V.J. Mokale, Design, synthesis and evaluation of antiinflammatory, analgesic and ulcerogenicity studies of novel S-substituted phenacyl-1, 3, 4-oxadiazole-2-thiol and Schiff bases of diclofenac acid as nonulcerogenic derivatives, Bioorg. Med. Chem. 16 (2008) 1822–1831.
[36] D. Raffa, B. Maggio, F. Plescia, S. Cascioferro, M.V. Raimondi, S. Plescia, M. G. Cusimano, Pyrazolo [3, 4-d] pyrimidine Derivatives as COX-2 Selective Inhibitors: Synthesis and Molecular Modelling Studies, Arch. Pharm. 342 (2009) 321–326.
[37] M.B. Palkar, A.S. Singhai, P.M. Ronad, A. Vishwanathswamy, T.S. Boreddy, V. P. Veerapur, M.S. Shaikh, R.A. Rane, R. Karpoormath, Synthesis, pharmacological screening and in silico studies of new class of Diclofenac analogues as a promising anti-inflammatory agents, Bioorg. Med. Chem. 22 (2014) 2855–2866.
[38] P.K. Singh, O. Silakari, Multitargeting Heterocycles: Improved and Rational Chemical Probes for Multifactorial Diseases, Key Heterocycle Cores for Designing Multitargeting Molecules, Elsevier2018, pp. 1-29.
[39] S. Pathania, P.K. Singh, Analyzing FDA-approved drugs for compliance of pharmacokinetic principles: should there be a critical screening parameter in drug designing protocols? Expert Opin. Drug Metab. Toxicol. 1–4 (2020).
[40] C.A. Winter, E.A. Risley, G.W. Nuss, Carrageenin-induced edema in hind paw of the rat as an assay for antiinflammatory drugs, Proc. Soc. Exp. Biol. Med. 111 (1962) 544–547.
[41] D. Pc, Studies on central nervous system depressants. (III). Influence of some tranquillizing agents on morphine analgesia, Arch. Int. Pharmacodyn. Ther. 141 (1963) 223–232.
[42] O. Davies, J. Raventos, A. Walpole, A method for the evaluation of analgesic activity using rats, Br. J. Pharmacol. Chemother. 1 (1946) 255.
[43] E.M. Ahmed, M.S. Hassan, A.A. El-Malah, A.E. Kassab, New pyridazine derivatives as selective COX-2 inhibitors and potential anti-inflammatory agents; design, synthesis and biological evaluation, Bioorg. Chem. 95 (2020), 103497.
[44] M. Djukic, M. Fesatidou, I. Xenikakis, A. Geronikaki, V.T. Angelova, V. Savic, M. Pasic, B. Krilovic, D. Djukic, B. Gobeljic, In vitro antioxidant activity of thiazolidinone derivatives of 1, 3-thiazole and 1, 3, 4-thiadiazole, Chem.-Biol. Interact. 286 (2018) 119–131.
[45] G. Bansal, S. Singh, V. Monga, P.V. Thanikachalam, P. Chawla, Synthesis and biological evaluation of thiazolidine-2, 4-dione-pyrazole conjugates as antidiabetic, anti-inflammatory and antioxidant agents, Bioorg. Chem. 92 (2019), 103271.
[46] E. Harder, W. Damm, J. Maple, C. Wu, M. Reboul, J.Y. Xiang, L. Wang, D. Lupyan, M.K. Dahlgren, J.L. Knight, OPLS3: a force field providing broad coverage of drug-like small molecules and proteins, J. Chem. Theory Comput. 12 (2016) 281–296.
[47] R.A. Friesner, R.B. Murphy, M.P. Repasky, L.L. Frye, J.R. Greenwood, T.A. Halgren, P.C. Sanschagrin, D.T. Mainz, Extra precision glide: Docking and scoring incorporating a model of hydrophobic enclosure for protein− ligand complexes, J. Med. Chem. 49 (2006) 6177–6196.
[48] L. Schrödinger, QikProp, version 3.5, New York, NY (2012).